

# Vibrational Spectroscopy of Reduced Re(I) Complexes of 1,10-Phenanthroline and Substituted Analogues

Sarah L. Howell and Keith C. Gordon\*

MacDiarmid Institute for Advanced Materials and Nanotechnology, Department of Chemistry, University of Otago, Union Place, Dunedin, New Zealand

Received: November 15, 2005; In Final Form: February 13, 2006

IR spectroscopy in concert with DFT calculations and resonance Raman spectroelectrochemistry has been used to identify the molecular orbital nature of the singly occupied molecular orbital (SOMO) in reduced  $[\text{Re}(\text{CO})_3\text{Cl}(\text{L})]$  and  $[\text{Re}(\text{CO})_3(4\text{-Mepy})(\text{L})]^+$  complexes, where L = 1,10-phenanthroline and its 4,7-diphenyl- and 3,4,7,8-tetramethyl-substituted analogues. The SOMO of each reduced species considered was found to be of  $b_1$  symmetry, rather than the close lying orbital of  $a_2$  symmetry (within a  $C_{2v}$  symmetry description of the phenanthroline moiety). This was deduced in a number of ways. First, the average carbonyl band force constants ( $\Delta k_{\text{av}} = k_{\text{av}}\{\text{reduced complex}\} - k_{\text{av}}\{\text{parent complex}\}$ ) range from  $-57$  to  $-41 \text{ N m}^{-1}$  for the series of compounds studied. The value of  $\Delta k_{\text{av}}$  relates to the extent of orbital overlap between the ligand MO and the metal  $d\pi$  MO. These values are consistent with population of a  $b_1$  MO because the wave function amplitude at the chelating nitrogens for this MO is significantly greater than that for  $a_2$  MO. Second, calculations on singly reduced  $[\text{Re}(\text{CO})_3(4\text{-Mepy})(\text{phen})]^+$  and  $[\text{Re}(\text{CO})_3(4\text{-Mepy})(\text{tem})]^+$  predict population of a  $b_2$  SOMO. The spectra predicted for these species are in close agreement with the vibrational spectroscopic data; for the IR data the shifts in the CO bands are predicted to  $6 \text{ cm}^{-1}$  and the mean absolute deviation between calculated and measured Raman bands was found to be  $10 \text{ cm}^{-1}$ .

## Introduction

1,10-Phenanthroline (phen) and substituted analogues are prevalent polypyridyl ligands.<sup>1</sup> Complexes of these ligands have been widely studied because of their interesting photophysical properties, such as long-lived metal-to-ligand charge transfer (MLCT) excited states.<sup>2</sup> Metal-to-ligand charge-transfer transitions as a first approximation involve the removal of an electron from a metal-based orbital ( $d\pi$ ) to one localized on the ligand ( $\pi^*$ ). Therefore, the nature of the ligand acceptor molecular orbital in the MLCT excited state is of interest.

Phen and substituted analogues have two close lying unoccupied molecular orbitals that are potentially populated in an optical transition. Kaim unambiguously demonstrated using EPR studies on the radical anion that the LUMO and LUMO+1 of phen have symmetries of  $b_1$  and  $a_2$  (Figure 1), respectively, within a  $C_{2v}$  symmetry description.<sup>3</sup> Since then, further EPR studies have been carried out by Kaim et al.<sup>4</sup> and Vlček et al.<sup>5</sup> on substituted phen, its derivatives and their complexes.

Kaim et al. showed that the correct ordering of the unoccupied molecular orbitals could be computationally predicted using Hartree–Fock and the 6-31G(d,p) basis set.<sup>4</sup> However, we have previously shown that a larger basis set is required (6-311+G(d,p)) when using the density functional theory hybrid method B3LYP.<sup>6</sup> In a study by Vlček et al. of  $[\text{W}(\text{CO})_4(\text{phen})]$  and  $[\text{W}(\text{CO})_4(\text{tem})]$ , TDDFT was used to calculate the lowest energy singlet and triplet state excitations.<sup>7</sup> Previously, Vlček et al. had shown through EPR experiments that the LUMO's of these complexes were of  $b_1$  and  $a_2$  symmetry, respectively.<sup>5</sup> They also used TDDFT to predict the transitions of these complexes. For  $[\text{W}(\text{CO})_4(\text{phen})]$  two low energy MLCT transitions are predicted. These occurred at 1.14 eV, corresponding

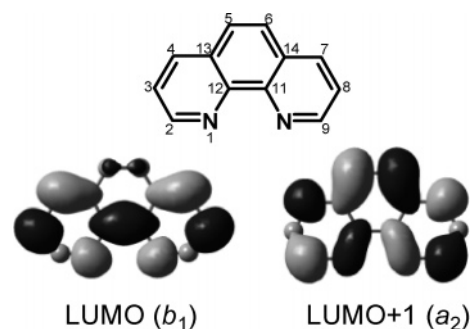


**Figure 1.** Atom labeling of phen along with the LUMO ( $b_1$ ) and LUMO+1 ( $a_2$ ). Hydrogen atoms have been omitted for clarity.

to a  $\text{W}(d\pi) \rightarrow \text{phen}(b_1)$  transition, and at 1.21 eV, corresponding to a  $\text{W}(d\pi) \rightarrow \text{phen}(a_2)$  transition. The calculation of  $[\text{W}(\text{CO})_4(\text{tem})]$  showed the accepting ligand  $\pi^*$  molecular orbitals to swap order. The lowest energy transition  $\text{W}(d\pi) \rightarrow \text{phen}(a_2)$  was predicted at 1.14 eV and the next highest energy transition  $\text{W}(d\pi) \rightarrow \text{phen}(b_1)$  at 1.26 eV.

The nature of the LUMO's of some polypyridyl ligands has been established using IR of the carbonyl region. Rhenium carbonyl complexes are ideal candidates to be studied by IR spectroscopy.<sup>8</sup> Carbonyl ligands have strong infrared bands at frequencies unobstructed by most solvents and the frequencies are indicative of the electron density at the metal. The assignment of the nature of the LUMO of a complex can be determined using IR spectroelectrochemistry of the reduced species. Different ligand based molecular orbitals have differing extents of communication with the metal moiety. Because the carbonyl frequencies are sensitive to the electron density at the metal center, the IR spectrum in the carbonyl region will differ depending on the molecular orbitals populated by reduction.

\* Corresponding author. E-mail: kgordon@alkali.otago.ac.nz.

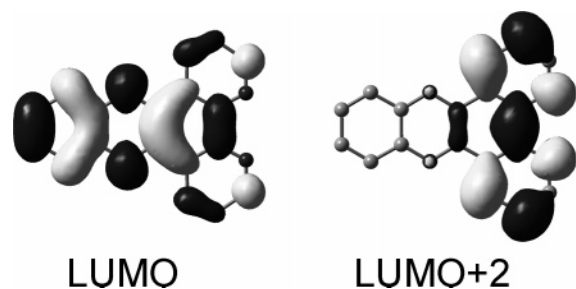


**Figure 2.** LUMO (phenazine-based) and LUMO+2 (phenanthroline-based) of dppz. Hydrogen atoms have been omitted for clarity.

It is also possible to examine the vibrational spectrum of the reduced ligand and thus establish the molecular orbital nature of the SOMO. This may be accomplished using resonance Raman spectroscopy on the reduced complex in which the excitation wavelength used to generate the Raman scattering is coincident with a chromophore of the ligand radical anion. The signature from the radical anion may be used to ascertain the structure of the species and infer the nature of the SOMO. This has been accomplished in a study of dppz complexes. In dppz there are two unoccupied molecular orbitals that lie close in energy and are quite different in terms of their disposition across the ligand framework. There is a phenanthroline-based molecular orbital that has significant wave function amplitude at the chelating nitrogen atoms (LUMO+2) and a phenazine based molecular orbital with no amplitude at the chelating nitrogen atoms but significant amplitude at the phenazine nitrogens (LUMO) (Figure 2). In a study of the  $[\text{Re}(\text{CO})_3\text{Cl}(\text{L})]$  complex of dppz and its partially and fully deuterated isotopomers,<sup>9</sup> the resonance Raman spectra of the reduced species were part of the evidence for a phenazine-based SOMO.

Computational chemistry can offer further insight into the structure and vibrational spectra of reduced complexes. Gordon et al. have carried out a number of DFT studies to model the Raman and IR spectra of singly reduced polypyridyl complexes in an attempt to establish the structural changes that occur upon reduction.<sup>9–12</sup>

In this study we have examined the vibrational spectra of a series of substituted phenanthroline complexes and their reduced species to ascertain the nature of the SOMO in each. The spectroscopic findings have been modeled using DFT calculations.

## Experimental Section

**Synthesis.** Preparation of  $[\text{Re}(\text{CO})_3\text{Cl}(\text{L})]$  complexes was based on the method by Moya et al.<sup>13</sup>  $[\text{Re}(\text{CO})_5\text{Cl}]$ , phen, dip and tem were used as supplied (Aldrich).

$[\text{Re}(\text{CO})_3\text{Cl}(\text{L})]$ :  $[\text{Re}(\text{CO})_5\text{Cl}]$  (0.298 g, 0.824 mmol) and polypyridyl ligand (0.824 mmol) were combined in argon purged methanol (100 mL) and refluxed under an argon atmosphere for 2½ h. The resulting solution was cooled and the precipitate collected. The solid was washed with methanol, diethyl ether and finally pentane.

$[\text{Re}(\text{CO})_3(4\text{-Mepy})(\text{L})]\text{CF}_3\text{SO}_3$  (where 4-Mepy is 4-methylpyridine) was made from  $[\text{Re}(\text{CO})_3\text{Cl}(\text{L})]$  on the basis of literature methods.<sup>14,15</sup>

$[\text{Re}(\text{CO})_3(4\text{-Mepy})(\text{L})]\text{CF}_3\text{SO}_3$ :  $[\text{Re}(\text{CO})_3\text{Cl}(\text{L})]$  (0.4 mmol) and  $\text{AgCF}_3\text{SO}_3$  (124 mg, 0.48 mmol) were dissolved in acetonitrile (100 mL). 4-Mepy was added (200 µL, 2.00 mmol) and the resulting mixture was then refluxed for 4 days. The solution was cooled and filtered to remove any AgCl. The solvent was removed from the filtrate by rotary evaporation, resulting in an oil. The oil was dissolved in either THF (phen

complex) or dichloromethane (tem complex) (100 mL). Pentane (100 mL) was added to this and the solution was placed in the refrigerator until fine needlelike crystalline solid formed from the solution.

**$[\text{Re}(\text{CO})_3\text{Cl}(\text{phen})]$ .** Yellow crystalline solid. Yield: 62%. <sup>1</sup>H NMR ( $\text{CDCl}_3$ , 300 MHz):  $\delta$  9.42 (dd, 2H,  $J_1 = 3.6$  Hz,  $J_2 = 1.5$  Hz), 8.57 (dd, 2H,  $J_1 = 6.9$  Hz,  $J_2 = 1.5$  Hz), 8.04 (s, 2H), 7.89 (dd, 2H,  $J_1 = 8.6$  Hz,  $J_2 = 5.1$  Hz).  $m/z$  451 ( $\{\text{M} - \text{Cl}\}^+$ ). Found: C, 37.38; H, 1.74; N, 5.78. Calcd for  $\text{C}_{15}\text{H}_8\text{N}_2\text{O}_3\text{ClRe}$ : C, 37.08; H, 1.66; N, 5.77.  $E^\circ$ (1st reduction) =  $-1.3$  V (vs DMFc/DMFc<sup>+</sup>).

**$[\text{Re}(\text{CO})_3\text{Cl}(\text{dip})]$ .** Orange crystalline solid. Yield: 80%. <sup>1</sup>H NMR ( $\text{CDCl}_3$ , 300 MHz):  $\delta$  9.44 (d, 2H,  $J = 5.4$  Hz), 8.05 (s, 2H), 7.80 (d, 2H,  $J = 5.4$  Hz), 7.62–7.52 (m, 10H). Found: C, 50.89; H, 2.71; N, 4.28. Calcd for  $\text{C}_{27}\text{H}_{16}\text{N}_2\text{O}_3\text{ClRe}$ : C, 50.82; H, 2.53; N, 4.39.  $E^\circ$ (1st reduction) =  $-1.2$  V (vs DMFc/DMFc<sup>+</sup>).

**$[\text{Re}(\text{CO})_3(4\text{-Mepy})(\text{phen})]\text{CF}_3\text{SO}_3$ .** Yellow crystalline solid. Yield: 95%. <sup>1</sup>H NMR (300 MHz,  $\text{CDCl}_3$ ):  $\delta$  9.55 (2H, dd,  $J_1 = 5.1$  Hz,  $J_2 = 1.2$  Hz), 8.84 (2H, dd,  $J_1 = 8.4$  Hz,  $J_2 = 1.5$  Hz), 8.20 (2H, s), 8.18 (2H, dd,  $J_1 = 8.1$  Hz,  $J_2 = 4.8$  Hz), 8.07 (2H, d,  $J = 6.6$  Hz), 7.08 (2H, d,  $J = 6.0$  Hz), 2.22 (3H, s).  $m/z$  544 ( $\{\text{M} - \text{CF}_3\text{SO}_3\}^+$ ). Found: C, 38.84; H, 2.30; N, 5.93. Calcd for  $\text{C}_{22}\text{H}_{15}\text{N}_3\text{O}_6\text{F}_3\text{SRe}(\text{C}_3\text{H}_{12})_{0.15}$ : C, 38.84; H, 2.41; N, 5.97%;  $E^\circ$ (1st reduction) =  $-1.3$  V (vs DMFc/DMFc<sup>+</sup>).

**$[\text{Re}(\text{CO})_3(4\text{-Mepy})(\text{tem})]\text{CF}_3\text{SO}_3$ .** Pale yellow crystalline solid. Yield: 55%. <sup>1</sup>H NMR (300 MHz,  $\text{CDCl}_3$ ):  $\delta$  9.11 (2H, s), 8.30 (2H, s), 7.98 (2H, d,  $J = 6.6$  Hz), 7.11 (2H, d,  $J = 6.3$  Hz), 2.88 (6H, s), 2.71 (6H, s), 2.22 (3H, s). Found: C, 41.65; H, 3.03; N, 5.42. Calcd for  $\text{C}_{26}\text{H}_{23}\text{N}_3\text{O}_6\text{F}_3\text{SRe}$ : C, 41.70; H, 3.10; N, 5.61.  $E^\circ$ (1st reduction) =  $-1.5$  V (vs DMFc/DMFc<sup>+</sup>).

**Physical Measurements.** Spectroscopic grade solvents were used for all spectroscopic measurements.

Spectral data were analyzed using Galactic Industries GRAMS/32 AI software.

<sup>1</sup>H NMR spectra were recorded at 25 °C, using either a Varian 300 MHz NMR spectrometer. Chemical shifts are given relative to residual solvent peaks. Microanalyses were performed at the Campbell Microanalysis Laboratory at the University of Otago. Mass spectrometry measurements were obtained from a Micromass LCT instrument for electrospray measurements or using a Shimadzu QP8000 alpha with ESI probe.

FT-IR spectra were collected, using a Perkin-Elmer Spectrum BX FT-IR system with Spectrum v.2.00 software.

A continuous-wave Melles Griot OmNichrome 543-MAP argon-ion laser was used to generate resonance Raman scattering. Typically, the laser output was adjusted to give 20–60 mW at the sample. The incident beam and the collection lens were arranged in a 135° backscattering geometry to reduce Raman intensity reduction by self-absorption.<sup>16</sup> An aperture-matched lens was used to focus scattered light through a narrow band line-rejection (notch) filter (Kaiser Optical Systems) and a quartz wedge (Spex) and onto the 100 µm entrance slit of a spectrograph (Acton Research SpectraPro 500i). The collected light was dispersed in the horizontal plane by a 1200 grooves/mm ruled diffraction grating (blaze wavelength 500 nm) and detected by a liquid nitrogen cooled back-illuminated Spec-10:100B CCD controlled by a ST-133 controller and WinSpec/32 (version 2.5.8.1) software (Roper Scientific). Wavenumber calibration was performed using Raman bands from a 1:1 (by volume) mixture of acetonitrile and toluene sample.<sup>17,18</sup> Peak positions were reproducible to within 1–2  $\text{cm}^{-1}$ . Spectra were obtained with a resolution of 5  $\text{cm}^{-1}$ . Freshly prepared samples were

held in a spinning NMR tube. Concentrations used were typically 5–20 mmol dm<sup>-3</sup>.

Electronic absorption spectra were recorded on a Varian Cary 500 scan UV–vis–NIR spectrophotometer, with Cary WinUV software. Samples were typically  $\sim 10^{-4}$  mol dm<sup>-3</sup>.

Cyclic voltammetry samples were freshly prepared in acetonitrile (1.0 mmol dm<sup>-3</sup>) with 0.1 mol dm<sup>-3</sup> tetrabutylammonium perchlorate. Samples were purged with nitrogen gas for 15 min prior to taking measurements. The electrochemical cell consisted of a 1.0 mm diameter platinum working electrode embedded in a Kel-F cylinder with a platinum auxiliary electrode and a Ag/AgCl reference electrode. The cyclic voltammograms were recorded using a Powerlab/4SP potentiostat with EChem v.1.5.2 software. Potentials were referenced to decamethylferrocene (DMFc).

Applied potentials reported are versus Ag/Ag<sup>+</sup>. The electronic absorption spectra of reduced species were measured using an OTTLE cell with a platinum grid as the working electrode.<sup>19</sup> Spectra were acquired by applying the first reduction potential of the complex to the sample and measuring approximately every two minutes. Difference spectra were found by subtracting the first spectrum from subsequent measurements for each compound. These were then added to the electronic absorption spectrum of the parent compound. For Raman spectra the OTTLE cell used had a Pt grid working electrode with a section cut out.<sup>20</sup> The Raman scattering was measured in this part of the cell to avoid laser reflection. The applied potential was set beyond the first reduction potential of the complex, and data were collected after sufficient time that the probed volume contained only the reduced product. The OTTLE cell used for IR spectroscopy is detailed elsewhere.<sup>21</sup> For some samples the spectra were measured using the minimum number of scans due to degradation.

### Calculations

The geometry, vibrational frequencies and their IR and Raman intensities were calculated using DFT calculations (B3LYP functional) with the basis sets: 6-31G(d) and LANL2DZ (on Re atoms). These were implemented with the Gaussian 03W<sup>22</sup> program package. No negative frequencies were predicted indicating that the structures obtained were at energy minima. The visualization of the vibrational modes was provided by GaussViewW (Gaussian Inc.).

### Results

The spectroscopic studies of the Re(I) complexes studied herein fall into two categories; first the carbonyl bands are probed using IR spectroelectrochemistry and second the ligand-based and ligand radical anion vibrations are examined with resonance Raman spectroscopy. DFT calculations have been carried out on the parent and reduced Re(I) complexes presented herein. The calculated frequencies are presented in Tables 2 and 3 and are considered in further detail in the discussion section. The DFT calculations carried out predicted the singly reduced Re(I) complexes considered in this study to be species with <sup>2</sup>B<sub>1</sub> symmetry.

**I. IR Spectra.** In Re(I) tricarbonyl complexes with a facial arrangement of carbonyls about the Re(I) center and with C<sub>3</sub> symmetry such as in the case of [Re(CO)<sub>3</sub>Cl(L)] complexes (L = bidentate ligand), three carbonyl bands are expected in the IR spectrum. From highest to lowest wavenumbers these have the symmetry labels a'(1), a'', and a'(2), respectively.<sup>23</sup> In complexes with three coordinated nitrogens, such as [Re(CO)<sub>3</sub>-(4-Mepy)(L)]<sup>+</sup>, the complex has pseudo-C<sub>3v</sub> symmetry, and therefore two of the modes become degenerate and the bands

**TABLE 1: Calculated, Observed and Literature Frequencies of Some Re(I) Polypyridyl Complexes**

complex	$\tilde{\nu}/\text{cm}^{-1}$		$k_{\text{av}}/\text{N m}^{-1}$	$\Delta k_{\text{av}}/\text{N m}^{-1}$ <sup>a</sup>	
	calculated	observed			
[Re(CO) <sub>3</sub> (phen)(4-Mepy)] <sup>+</sup>	1929 <sup>b</sup>	2035	1559		
calculated	1942	1953	2020		
[Re(CO) <sub>3</sub> (phen <sup>•-</sup> )(4-Mepy)]	1896	1889	2099	1502	-57
calculated	1899	1917	1990		
[Re(CO) <sub>3</sub> (tem)(4-Mepy)] <sup>+</sup>	1925 <sup>b</sup>	2032	1553		
calculated	1927	1948	2017		
[Re(CO) <sub>3</sub> (tem <sup>•-</sup> )(4-Mepy)]	1896 <sup>b</sup>	2012	1513	1513	-41
calculated	1895	1913	1986		
[Re(CO) <sub>3</sub> Cl(phen)]	1901	1918	2023	1533	
calculated	1910	1931	1999		
[Re(CO) <sub>3</sub> Cl(phen <sup>•-</sup> )] <sup>-</sup>	1871 <sup>b</sup>	1999	1480	1480	-52
calculated	1873	1887	1969		
[Re(CO) <sub>3</sub> Cl(dip)]	1901	1917	2022	1531	
calculated	1908	1929	1997		
[Re(CO) <sub>3</sub> Cl(dip <sup>•-</sup> )] <sup>-</sup>	1869	1886	2000	1487	-44
calculated	1876	1891	1971		
[Re(4,4'-(CO <sub>2</sub> Et) <sub>2</sub> bpy)(CO) <sub>3</sub> (4-Etpy)] <sup>+</sup> <sup>c</sup>	1935 <sup>b</sup>	2038	1567		
[Re(4,4'-(CO <sub>2</sub> Et) <sub>2</sub> bpy <sup>•-</sup> )(CO) <sub>3</sub> (4-Etpy)] <sup>-</sup> <sup>c</sup>	1905 <sup>b</sup>	2015	1524	1524	-44
[Re(4,4'-(CO <sub>2</sub> Et) <sub>2</sub> bpy)(CO) <sub>3</sub> (MQ <sup>+</sup> )] <sup>2+</sup> <sup>c</sup>	1939 <sup>b</sup>	2039	1572		
[Re(4,4'-(CO <sub>2</sub> Et) <sub>2</sub> bpy)(CO) <sub>3</sub> (MQ <sup>+</sup> )] <sup>2+</sup> <sup>c</sup>	1939 <sup>b</sup>	2039	1572		
[Re(4,4'-(CO <sub>2</sub> Et) <sub>2</sub> bpy)(CO) <sub>3</sub> (MQ <sup>•+</sup> )] <sup>+</sup> <sup>c</sup>	1928 <sup>b</sup>	2032	1557	1557	-15
[Re(4,4'-bpy) <sub>2</sub> (CO) <sub>3</sub> Cl] <sup>d</sup>	2026	1922	1895	1533	
[Re(4,4'-bpy <sup>•-</sup> ) <sub>2</sub> (CO) <sub>3</sub> Cl] <sup>-</sup> <sup>d</sup>	2012	1903	1882	1509	-24

<sup>a</sup>  $\Delta k_{\text{av}}$  upon reduction. <sup>b</sup> Bands appear broad and are assigned as e symmetry, thus doubly degenerate. <sup>c</sup> Reference 28. <sup>d</sup> Reference 31.

**TABLE 2: Calculated and Observed Band Frequencies for Singly Reduced [Re(CO)<sub>3</sub>(4-Mepy)(phen)]<sup>+</sup>**

$\nu^a$	symmetry <sup>b</sup>	[Re(CO) <sub>3</sub> (4-Mepy)(phen <sup>•-</sup> )]	[Re(CO) <sub>3</sub> (4-Mepy)(phen <sup>•-</sup> )]
		B3LYP/6-31G(d) <sup>c</sup> $\tilde{\nu}/\text{cm}^{-1}$	experimental <sup>d</sup> $\tilde{\nu}/\text{cm}^{-1}$
69	a <sub>1</sub> (4-Mepy)	1008	1018
72	a <sub>1</sub> (4-Mepy)	1064	1062
74	a <sub>1</sub>	1076	1093
77	a <sub>1</sub>	1139	1146
78	a <sub>1</sub>	1185	1161
82	a <sub>1</sub>	1225	1221
85	b <sub>2</sub> (4-Mepy)	1272	1278
86	a <sub>1</sub>	1292	1309
89	a <sub>1</sub> (4-Mepy)	1399	1389
90	b <sub>2</sub>	1403	1410
91	a <sub>1</sub>	1421	1431
95	a <sub>1</sub>	1460	1445
97	a <sub>1</sub> (4-Mepy)	1471	1489
99	a <sub>1</sub> (4-Mepy)	1507	1511
100	a <sub>1</sub>	1532	1534
104	a <sub>1</sub>	1605	1578
105	a <sub>1</sub> (4-Mepy)	1626	1626

<sup>a</sup> Mode numbers are from the calculation. <sup>b</sup> Symmetries are based on C<sub>2v</sub> symmetry of phen and are phen localized unless otherwise indicated. <sup>c</sup> The LANL2DZ basis set was used for the Re atom. <sup>d</sup> Resonance Raman data were collected with 514.5 nm excitation. Due to the large number of bands observed only those with intensities of >20% of the most intense band ( $\nu_{100}$ ) are tabulated.

have the labels a<sub>1</sub> and e. Upon reduction or excitation the coordinated nitrogens become inequivalent, reducing the symmetry to C<sub>s</sub> and hence lifting the degeneracy of the modes.<sup>24,25</sup>

The  $\Delta A$  IR spectrum of [Re(CO)<sub>3</sub>(4-Mepy)(phen<sup>•-</sup>)] – [Re(CO)<sub>3</sub>(4-Mepy)(phen)]<sup>+</sup>, is shown in Figure 3a. Parent complex carbonyl bands are evident at 1929 and 2035 cm<sup>-1</sup> as bleaches in the spectrum (Table 1). Upon reduction of [Re(CO)<sub>3</sub>(4-Mepy)(phen)]<sup>+</sup> the carbonyl bands shift to lower frequencies. The 1929 cm<sup>-1</sup> band of the parent species is resolved into two bands, at 1886 and 1889 cm<sup>-1</sup>, in the spectrum of the reduced complex. The carbonyl band in the spectrum of the parent complex at 2035 cm<sup>-1</sup> is shifted to 2009 cm<sup>-1</sup> in the spectrum of the reduced complex. This decrease in frequency of the carbonyl bands upon reduction is consistent with the

TABLE 3: Calculated and Observed Band Frequencies for Reduced  $[\text{Re}(\text{CO})_3(4\text{-Mepy})(\text{tem})]^+$ 

experimental <sup>a</sup>	symmetry <sup>b</sup>	$[\text{Re}(\text{CO})_3(4\text{-Mepy})(\text{tem}^{\bullet-})]$ B3LYP/6-31G(d) <sup>c</sup> $\tilde{\nu}/\text{cm}^{-1}$	$[\text{Re}(\text{CO})_3(4\text{-Mepy})(\text{tem}^{\bullet-})]$ experimental <sup>d</sup> $\tilde{\nu}/\text{cm}^{-1}$
96	$a_1(4\text{-Mepy})$	1211	1208
102	$a_1$	1285	1307
104	$a_1$	1338	1339
114	$a_1$	1435	1427
116	$a_1$	1464	
117	$a_1$	1465	
118	$a_1(\text{tem} + 4\text{-Mepy})$	1469	1444
119	$a_1(\text{tem} + 4\text{-Mepy})$	1469	
128	$a_1(\text{tem} + 4\text{-Mepy})$	1509	1525
130	$a_1$	1548	1557
132	$a_1$	1601	1599
133	$a_1(4\text{-Mepy})$	1626	1616

<sup>a</sup> Mode numbers are from the calculation. <sup>b</sup> Symmetries are based on  $C_{2v}$  symmetry of the phenanthroline moiety of tem and are tem localized unless otherwise indicated. <sup>c</sup> The LANL2DZ basis set was used for the Re atom. <sup>d</sup> Resonance Raman data were collected with 457.9 nm excitation.

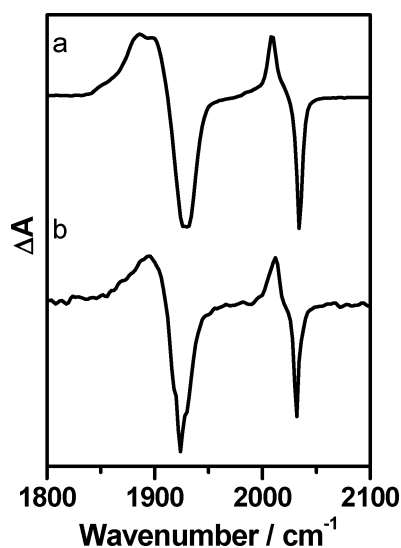


Figure 3.  $\Delta A$  IR spectra upon reduction of (a)  $[\text{Re}(\text{CO})_3(4\text{-Mepy})(\text{phen})]^+$  and (b)  $[\text{Re}(\text{CO})_3(4\text{-Mepy})(\text{tem})]^+$ .

occupation of a  $\pi^*$  molecular orbital of phen. Increase in the electron density in the  $\pi^*$  molecular orbital of phen increases the back-bonding to the  $\pi^*$  molecular orbital of the carbonyl ligands, resulting in a decrease in frequency.

The  $\Delta A$  IR spectrum measured of the complex  $[\text{Re}(\text{CO})_3(4\text{-Mepy})(\text{tem}^{\bullet-})] - [\text{Re}(\text{CO})_3(4\text{-Mepy})(\text{tem})]^+$  upon application of a reduction potential is shown in Figure 3b. Similar to the data for  $[\text{Re}(\text{CO})_3(4\text{-Mepy})(\text{phen})]^+$ , bleaching of the carbonyl bands of the parent complex is observed at 1925 and 2032  $\text{cm}^{-1}$  (Table 1). Concomitant with this, new features grow in at 1896 and 2012  $\text{cm}^{-1}$ . The 1925 and 1896  $\text{cm}^{-1}$  bands have significantly greater bandwidth than those at 2032 and 2012  $\text{cm}^{-1}$ . The lower frequency pair (1925 and 1896  $\text{cm}^{-1}$ ) are attributed to the  $e$  modes of the carbonyl system and those at 2032 and 2012  $\text{cm}^{-1}$  are  $a_1$  modes.

The IR spectrum of  $[\text{Re}(\text{CO})_3\text{Cl}(\text{phen})]$  has carbonyl bands at 1901, 1917, and 2022  $\text{cm}^{-1}$  (Table 1). The reduced species has bands at 1871 and 1999  $\text{cm}^{-1}$ , with the former being of greater bandwidth than the latter.

Upon application of a reduction potential the IR spectrum of  $[\text{Re}(\text{CO})_3\text{Cl}(\text{dip})]$  has bleaches at 1901, 1917, and 2022  $\text{cm}^{-1}$  (Table 1) due to the carbonyl modes of the parent species. The IR spectrum of  $[\text{Re}(\text{CO})_3\text{Cl}(\text{dip}^{\bullet-})]^-$  has carbonyl bands at 1869, 1886 and 2000  $\text{cm}^{-1}$ .

**II. Resonance Raman Spectra.** An excitation wavelength of 514.5 nm was used to measure the resonance Raman spectrum

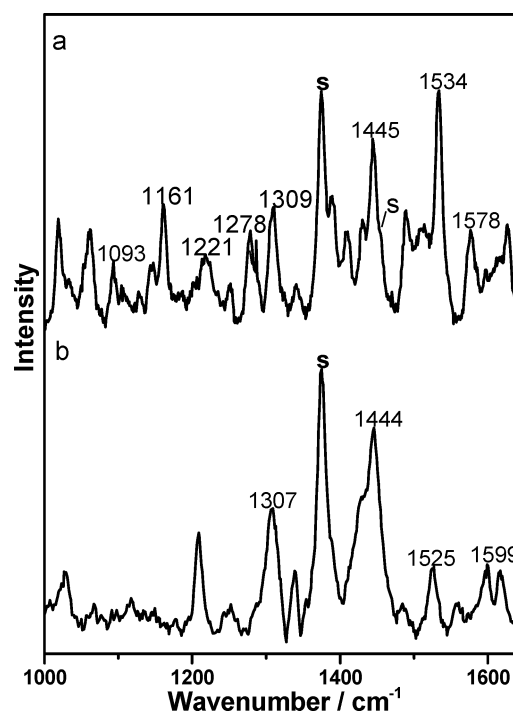


Figure 4. Resonance Raman spectrum of singly reduced (a)  $[\text{Re}(\text{CO})_3(4\text{-Mepy})(\text{phen})]^+$  ( $\lambda_{\text{ex}} = 514.5$  nm) and (b)  $[\text{Re}(\text{CO})_3(4\text{-Mepy})(\text{tem})]^+$  ( $\lambda_{\text{ex}} = 457.9$ ) in acetonitrile (0.1 M TBAP as supporting electrolyte).

of  $[\text{Re}(\text{CO})_3(4\text{-Mepy})(\text{phen}^{\bullet-})]$  (Figure 4a). The spectrum of the parent species (spectrum not shown) at 514.5 nm is dramatically different to that of the reduced species. The parent species is not in resonance at this excitation wavelength so the spectrum is dominated by solvent bands. The spectrum has two weak bands at 1061 and 1305  $\text{cm}^{-1}$ . Although in the spectrum of the reduced complex there are bands close to these positions (1062 and 1309  $\text{cm}^{-1}$ ), the intensities of these bands have clearly increased relative to the solvent bands and there is growth of a large number of new bands as the sample is reduced. A number of bands are observed in the resonance Raman spectrum of  $[\text{Re}(\text{CO})_3(4\text{-Mepy})(\text{phen}^{\bullet-})]$ , these have been tabulated in Table 2.

An excitation wavelength of 457.9 nm was used to collect the resonance Raman spectrum of singly reduced  $[\text{Re}(\text{CO})_3(4\text{-Mepy})(\text{tem})]^+$ . The spectrum of the parent complex is of an emission background with only one weak discernible feature—a band at 1376  $\text{cm}^{-1}$  due to the solvent (spectrum not shown). The resonance Raman spectrum of  $[\text{Re}(\text{CO})_3(4\text{-Mepy})(\text{tem}^{\bullet-})]$

has eight bands observed in the 1000–1650  $\text{cm}^{-1}$  region of the spectrum (Figure 4b, Table 2).

## Discussion

**I. IR Spectra.** The carbonyl band frequencies are sensitive to the environment at the metal center due to back-bonding from the metal center to the carbonyl ligands. Changes in the frequencies of the carbonyl bands upon reduction in the phen, dip and tem complexes may be used to determine the nature of the SOMO. Occupation of the  $b_1$  molecular orbital will allow the reducing electron to have greater overlap with the metal center compared to the  $a_2$  orbital due to the greater electron density on the coordinating nitrogens.

One way to quantify the extent of back-bonding in these types of complexes is to calculate the average carbonyl force constants ( $k_{\text{av}}$ ) for the parent and reduced species and examine the change upon reduction ( $\Delta k_{\text{av}}$ ).  $k_{\text{av}}$  is calculated using eq 1,<sup>26,27</sup> and the values are presented in Table 1. This approach, developed by Stufkens et al.,<sup>27</sup> has recently been employed by Gordon et al. to investigate the localization of the SOMO in reduced Re(I) tricarbonyl complexes of biquinoline and other closely related polypyridyl ligands.<sup>21</sup>

$$k_{\text{av}} = 4.0383 \times 10^{-4} \frac{\sum_i g_i \nu_i^2}{\sum_i g_i} \quad (1)$$

where  $g_i$  = degeneracy of the  $i$ th CO-stretching mode and  $\nu_i$  is the frequency of the  $i$ th CO-stretching mode ( $\text{cm}^{-1}$ ).

The change in  $k_{\text{av}}$  ( $\Delta k_{\text{av}}$ ) values upon reduction ( $k_{\text{av}}(\text{reduced}) - k_{\text{av}}(\text{parent})$ ) of the substituted phen complexes and a number of reference compounds can be used to qualitatively ascertain the extent of communication between the ligand and metal in each reduced complex and therefore deduce the nature of the SOMO.

Meyer et al. investigated the complexes  $[\text{Re}(4,4'-(\text{CO}_2\text{Et})_2\text{-bpy})(\text{CO})_3(4\text{-Etpy})]^+$  and  $[\text{Re}(4,4'-(\text{CO}_2\text{Et})_2\text{bpy})(\text{CO})_3(\text{MQ}^+)]^{2+}$  ( $4,4'-(\text{CO}_2\text{Et})_2\text{bpy} = 4,4'$ -bis(ethylethanoate)-2,2'-bipyridine; 4-Etpy = 4-ethylpyridine;  $\text{MQ}^+ = N$ -methyl-4,4'-bipyridinium cation).<sup>28</sup> The reduced forms of each of these two complexes exemplify the two extremes—good and poor communication to the metal center. The reduced species were formed upon by photoexcitation followed by reductive quenching with 10-methylphenothiazine (10-MePTZ). In the resulting singly reduced  $[\text{Re}(4,4'-(\text{CO}_2\text{Et})_2\text{bpy})(\text{CO})_3(4\text{-Etpy})]^+$ , a bpy-based molecular orbital is occupied. The bpy-based molecular orbital is of  $b_1$  symmetry and closely resembles that of the  $b_1$  LUMO of phen.<sup>2,29,30</sup> The resulting singly reduced  $[\text{Re}(4,4'-(\text{CO}_2\text{Et})_2\text{bpy})(\text{CO})_3(\text{MQ}^+)]^{2+}$ , formed by reaction of the photoproduct with a reductive quencher, has the reducing electron on the  $\text{MQ}^+$  ligand. This reducing electron is localized on the remote pyridinium ring, resulting in a Re(I) center bridged by a pyridyl to a reduced pyridinium. The separation of the reduced electron from the metal center results in very little communication and hence a small change in the extent of back-bonding is expected.

In the case of  $[\text{Re}(4,4'-(\text{CO}_2\text{Et})_2\text{bpy})(\text{CO})_3(4\text{-Etpy})]^+$  the  $k_{\text{av}}$  is calculated at 1567  $\text{N m}^{-1}$ , on the basis of a doubly degenerate mode at 1935  $\text{cm}^{-1}$  and a singly degenerate mode at 2038  $\text{cm}^{-1}$ .<sup>28</sup> For  $[\text{Re}(4,4'-(\text{CO}_2\text{Et})_2\text{bpy}^*)(\text{CO})_3(4\text{-Etpy})]$  the  $k_{\text{av}}$  is 1524  $\text{N m}^{-1}$ , calculated from modes at 1905 (e) and 2015 ( $a_1$ )  $\text{cm}^{-1}$ .  $\Delta k_{\text{av}}$  upon reduction of this complex is  $-44 \text{ N m}^{-1}$ . For  $[\text{Re}(4,4'-(\text{CO}_2\text{Et})_2\text{bpy})(\text{CO})_3(\text{MQ}^+)]^{2+}$ ,  $k_{\text{av}}$  is calculated at 1572

$\text{N m}^{-1}$ . Upon reduction there is a  $\Delta k_{\text{av}}$  of  $-15 \text{ N m}^{-1}$ . The smaller  $\Delta k_{\text{av}}$  upon reduction is indicative of a smaller change in back-bonding compared to the complex  $[\text{Re}(4,4'-(\text{CO}_2\text{Et})_2\text{-bpy})(\text{CO})_3(4\text{-Etpy})]^+$ .

For the complex  $[\text{Re}(4,4'\text{-bpy})_2(\text{CO})_3\text{Cl}]$ , the IR spectrum of the parent and reduced complex have been measured.<sup>31</sup> The  $\Delta k_{\text{av}}$  has been calculated at  $-24 \text{ N m}^{-1}$ ,<sup>21</sup> from the data collected by George et al.,<sup>31</sup> approximately half that of  $[\text{Re}(\text{bpy})(\text{CO})_3\text{Cl}]$ , which was calculated as  $-44 \text{ N m}^{-1}$ .<sup>27</sup> The small  $\Delta k_{\text{av}}$  for reduction of  $[\text{Re}(4,4'\text{-bpy})_2(\text{CO})_3\text{Cl}]$  is attributed to the localization of the acceptor molecular orbital on the monodentate ligand 4,4'-bpy, which can communicate with the metal via a single coordinated nitrogen, hence transfer from the reduced ligand to the metal center is less.

Singly reduced phen had been shown to be a species with  ${}^2B_1$  symmetry.<sup>3</sup> The presence of a metal center leads to a preferential stabilization of the  $b_1$  unoccupied molecular orbital over that of  $a_2$  symmetry. This stabilization reduces the configuration interaction between the close lying unoccupied molecular orbitals.<sup>4,32</sup>  $[\text{Re}(\text{CO})_3\text{Cl}(\text{phen})]$  and  $[\text{Re}(\text{CO})_3(4\text{-Mepy})(\text{phen}^*)]$  are species with  ${}^2B_1$  symmetry, therefore should have a  $\Delta k_{\text{av}}$  for reduction comparable to that calculated for  $[\text{Re}(4,4'-(\text{CO}_2\text{Et})_2\text{bpy})(\text{CO})_3(4\text{-Etpy})]^+$  or for  $[\text{Re}(\text{bpy})(\text{CO})_3\text{Cl}]$ . Upon the reduction of  $[\text{Re}(\text{CO})_3(4\text{-Mepy})(\text{phen})]^+$   $k_{\text{av}}$  decreases from 1559 to 1502  $\text{N m}^{-1}$ , a decrease of 57  $\text{N m}^{-1}$ . For  $[\text{Re}(\text{CO})_3\text{Cl}(\text{phen})]$ , the  $\Delta k_{\text{av}}$  was calculated to be  $-52 \text{ N m}^{-1}$ . Both phen complexes have  $\Delta k_{\text{av}}$  values for reduction of slightly greater magnitude than the  $\Delta k_{\text{av}}$  upon reduction of  $[\text{Re}(4,4'-(\text{CO}_2\text{Et})_2\text{bpy})(\text{CO})_3(4\text{-Etpy})]^+$  or  $[\text{Re}(\text{bpy})(\text{CO})_3\text{Cl}]$ .

The ordering of the molecular orbitals can be changed by varying the substituents on phen. Kaim et al. studied the potassium salts for the reduced ligands, 2,2'-bipyridine, 4,4'-dimethyl-2,2'-bipyridine 1,10-phenanthroline, and 4,7-dimethyl-1,10-phenanthroline. From the EPR data of these reduced species they invoked  $b_1$  orbital symmetry for the SOMO.<sup>3</sup> The radical anion of several diaza derivatives of phen and their  $\{\text{M}(\text{CO})_4\}$  complexes ( $\text{M} = \text{Cr}, \text{Mo}, \text{W}$ ) have been considered,<sup>4</sup> as well as methyl substituted phen and their Pt(II) complexes,<sup>33</sup> to determine the  $b_1/a_2$  molecular orbital ordering. The nature of the LUMO of tem and some of its complexes has been investigated by the groups of Kaim<sup>32,33</sup> and Vlček.<sup>5,7</sup> Substitution at the 3, 4, 7, and 8 positions of the phenanthroline moiety cause a switching of molecular orbitals from unsubstituted phen:  $\text{tem}^-$  is a species with  ${}^2A_2$  symmetry, as determined by Kaim et al. through EPR studies.<sup>32</sup> Complexation can potentially induce orbital swapping as the metal center will stabilize the  $b_1$  orbital more than the  $a_2$  orbital. Coordination of tem to  $\{\text{Pt}(\text{Mes})_2\}^{2+}$  ( $\text{Mes} = \text{mesityl}$ ),<sup>32,33</sup>  $\{\text{Cr}(\text{CO})_4\}^5$  and  $\{\text{W}(\text{CO})_4\}^5$  was investigated and these complexes were all found to have LUMO's of  $a_2$  symmetry. Solvent-induced orbital switching was found for the Pt(II) complex upon changing the solvent from THF to the polar solvent DMF, evidenced by EPR studies.<sup>33</sup>

For  $[\text{Re}(\text{CO})_3(4\text{-Mepy})(\text{tem})]^+$ , the  $\Delta k_{\text{av}}$  upon reduction is calculated at  $-41 \text{ N m}^{-1}$ , less than that calculated for  $[\text{Re}(\text{CO})_3(4\text{-Mepy})(\text{phen})]^+$ , but comparable to that calculated for  $[\text{Re}(4,4'-(\text{CO}_2\text{Et})_2\text{bpy})(\text{CO})_3(4\text{-Etpy})]^+$  and much larger than for  $[\text{Re}(4,4'-(\text{CO}_2\text{Et})_2\text{bpy})(\text{CO})_3(\text{MQ}^+)]^{2+}$ . Therefore, it is likely that the LUMO of the tem complex is predominantly  $b_1$ .

Although dip does not appear to have been studied, it has been postulated that because the localization of the molecular orbital at the 4 and 7 positions are similar for both the  $b_1$  and  $a_2$  molecular orbitals (Figure 1), the stabilization of the molecular orbitals induced by substitution at these positions would be similar, therefore no orbital switching would occur.<sup>5</sup> This would

suggest that  $\text{dip}^{\bullet-}$  is a species with  ${}^2\text{B}_1$  symmetry. The  $\Delta k_{\text{av}}$  for reduction of  $[\text{Re}(\text{CO})_3\text{Cl}(\text{dip})]$  was calculated to be  $-44 \text{ N m}^{-1}$ . This is a very similar value to that observed for the phen complex and it supports the assignment of the SOMO of  $[\text{Re}(\text{CO})_3\text{Cl}(\text{dip})]$  as a  $b_1$  molecular orbital.

Modeling was undertaken to determine how well DFT calculations are able to predict the changes in electron density at the metal center. Frequency calculations were used as these provide ready comparison between calculated and experimental observables. Due to the overestimate of vibrational frequencies by an average of over  $100 \text{ cm}^{-1}$  by the calculations it is appropriate to introduce a scale factor.<sup>34</sup> Due to the higher anharmonicity of carbonyl modes relative to C–C ligand modes,<sup>26</sup> the two spectral regions require different scale factors. For the polypyridyl region ( $1000\text{--}1650 \text{ cm}^{-1}$ ) a scale factor of 0.97 is appropriate; however, for the carbonyl bands a scale factor of 0.95 minimizes the absolute deviation between experimental and calculated frequencies.

The mean absolute deviation between observed and calculated carbonyl mode frequencies for the parent and reduced complexes was found to be  $16 \text{ cm}^{-1}$ . More importantly, the shifts in the positions of the carbonyl bands upon reduction of the complexes were predicted with a mean absolute deviation between observed and calculated shifts of  $6 \text{ cm}^{-1}$ .

For  $[\text{Re}(\text{CO})_3(4\text{-Mepy})(\text{phen})]^+$  ground-state carbonyl bands are observed at  $1929$  and  $2035 \text{ cm}^{-1}$  with modes predicted at  $1942$ ,  $1953$ , and  $2020 \text{ cm}^{-1}$  (Table 1). Upon reduction the bands are observed to decrease by  $43$ ,  $40$  and  $26 \text{ cm}^{-1}$ , respectively. The predicted decreases are within  $4 \text{ cm}^{-1}$  of those observed.

For the tem complex,  $[\text{Re}(\text{CO})_3(4\text{-Mepy})(\text{tem})]^+$ , the bands are slightly decreased in frequency, compared to  $[\text{Re}(\text{CO})_3(4\text{-Mepy})(\text{phen})]^+$ , at  $1925$  and  $2032 \text{ cm}^{-1}$ . This decrease is predicted by the calculation with modes at  $1937$ ,  $1948$ , and  $2017 \text{ cm}^{-1}$  (Table 1). A decrease in the frequencies of the bands by  $29$  and  $20 \text{ cm}^{-1}$  is observed upon reduction. The calculated shifts are all too large at  $42$ ,  $35$ , and  $31 \text{ cm}^{-1}$  for the three modes. The smaller than predicted shifts observed may be indicative of the molecular orbital occupied by the reducing electron having some  $a_2$  character.

For the  $[\text{Re}(\text{CO})_3\text{Cl}(\text{phen})]$  and  $[\text{Re}(\text{CO})_3\text{Cl}(\text{dip})]$  complexes, carbonyl bands are observed at the same frequency, within experimental uncertainty, at  $1901$ ,  $1918$ , and  $2023 \text{ cm}^{-1}$ . These are predicted at  $1910$ ,  $1931$ , and  $1999 \text{ cm}^{-1}$  for  $[\text{Re}(\text{CO})_3\text{Cl}(\text{phen})]$  (Table 1). The calculation of the dip complex predicts each band within  $2 \text{ cm}^{-1}$  of that calculated for the phen complex. In the reduced form the carbonyl bands of the phen complex shift to  $1871$  and  $1999 \text{ cm}^{-1}$ . The dip complex has two bands within experimental uncertainty at  $1869$  and  $2000 \text{ cm}^{-1}$ , with an additional band at  $1886 \text{ cm}^{-1}$ . The calculated frequencies of the carbonyl bands for  $[\text{Re}(\text{CO})_3\text{Cl}(\text{phen}^{\bullet-})]^-$  are  $1873$ ,  $1887$ , and  $1969 \text{ cm}^{-1}$ . The reduced dip complex has the lowest and highest energy carbonyl bands predicted within  $3 \text{ cm}^{-1}$  of those for the phen complex. However, the middle band is predicted at  $1891 \text{ cm}^{-1}$ . This predicted difference of  $4 \text{ cm}^{-1}$  manifests as splitting of the two degenerate modes for the dip complex, resulting in three, not two, bands in the reduced complex.

**II. Resonance Raman Spectra.** Resonance Raman spectroscopy has been used to probe the  $1000\text{--}1650 \text{ cm}^{-1}$  region, as bands from the supporting electrolyte swamps infrared spectra in this region. Because the electrolyte bands are not resonantly enhanced at the excitation wavelengths used, the electrolyte is spectroscopically silent in the region of interest and the spectra of the reduced species more readily collected than with IR spectroscopy. The excitation wavelength is chosen such that

the reduced species, but not the parent complexes, are enhanced. The appropriate excitation wavelength was chosen by considering the electronic absorption spectra of the reduced species (see Supporting Information).

The resonance Raman spectra of the reduced  $[\text{Re}(\text{CO})_3\text{Cl}(\text{L})]$  complexes were unable to be considered in using the experimental protocol described in this paper as reduction of the  $[\text{Re}(\text{CO})_3\text{Cl}(\text{L})]$  complexes of phen, dip and tem via application of a reduction potential results in the rapid formation of a number of potential byproducts.<sup>35</sup> Although electronic absorption and resonance Raman spectra of the reduced species takes a number of minutes to collect, the IR spectrum of the reduced complexes can be collected within several seconds. This acquisition time is sufficiently short to measure the signal due to the reduced complexes before appreciable secondary reactions take place. The resulting spectra are comparatively noisy; however, the frequencies of the carbonyl bands were able to be identified. In the first several seconds the growth of 2–3 bands due to carbonyl modes are observed, suggesting the formation of a single species. Over a longer period of time (a couple of minutes) the spectra show a change in the number of bands of positive?  $\Delta A$  (not shown). This is indicative of the formation of more than one species in solution. This does not occur for the  $[\text{Re}(\text{CO})_3(4\text{-Mepy})(\text{L})]^+$  complexes as the 4-Mepy ligand is less labile than  $\text{Cl}^-$ .

The bands observed in the resonance Raman spectrum of  $[\text{Re}(\text{CO})_3(4\text{-Mepy})(\text{phen}^{\bullet-})]$  can also be compared to those in the resonance Raman spectra of  $\text{Li}^+\text{phen}^{\bullet-}$ , reported by Leroi et al.<sup>36</sup> and Schoonover et al.<sup>37</sup> It must be noted that these previously published studies were carried out at different excitation wavelengths to the  $514.5 \text{ nm}$  excitation considered herein. The spectrum collected by Schoonover et al.<sup>37</sup> used  $406.7 \text{ nm}$  excitation and the spectra collected by Leroi et al.<sup>36</sup> were measured with a series of excitation wavelengths:  $351.1$ ,  $363.8$ ,  $406.8$ ,  $568$ , and  $647 \text{ nm}$ . The resonance enhancement pattern for those  $\text{Li}^+\text{phen}^{\bullet-}$  spectra is expected to be different to that observed using  $514.5 \text{ nm}$  excitation of  $[\text{Re}(\text{CO})_3(4\text{-Mepy})(\text{phen}^{\bullet-})]$ . Hence, comparison of band intensities would be invalid and some bands may be enhanced in one spectrum and not appear at all in another. However, the vibrational frequencies are not modulated allowing the comparison of frequencies to be carried out. The bands at  $1221$ ,  $1410$ ,  $1445$ ,  $1534$ , and  $1578 \text{ cm}^{-1}$  in the resonance Raman spectrum of  $[\text{Re}(\text{CO})_3(4\text{-Mepy})(\text{phen}^{\bullet-})]$  are likely to be due to the same modes that produce bands at  $1221$ ,  $1405$ ,  $1449$ ,  $1539$ , and  $1576 \text{ cm}^{-1}$ , respectively, in the spectra of  $\text{Li}^+\text{phen}^{\bullet-}$ , measured by Leroi et al.<sup>36</sup> The band at  $1431 \text{ cm}^{-1}$  in the spectrum of  $[\text{Re}(\text{CO})_3(4\text{-Mepy})(\text{phen}^{\bullet-})]$  can be correlated to the  $\text{Li}^+\text{phen}^{\bullet-}$  band observed by Schoonover et al. at  $1421 \text{ cm}^{-1}$ .<sup>37</sup> Both studies report a number of additional  $\text{Li}^+\text{phen}^{\bullet-}$  bands that cannot be readily correlated to the bands observed in the resonance Raman spectrum of  $[\text{Re}(\text{CO})_3(4\text{-Mepy})(\text{phen}^{\bullet-})]$ , for example the prominent bands at  $1130$ ,  $1272$ , and  $1585 \text{ cm}^{-1}$  observed by Schoonover et al.<sup>37</sup> However, the lack of enhancement of these modes in the resonance Raman spectrum of  $[\text{Re}(\text{CO})_3(4\text{-Mepy})(\text{phen}^{\bullet-})]$  may be due to an absence of enhancement of these bands at this particular wavelength.<sup>38</sup>

Gordon et al. reported the resonance Raman spectrum of the metal-to-ligand charge-transfer excited state of  $[\text{Cu}(\text{phen})(\text{PPh}_3)_2]^+$ , which can be denoted as  $[\text{Cu}^{\text{II}}(\text{phen}^{\bullet-})(\text{PPh}_3)_2]^{+*}$ . Three bands were observed, which were assigned to  $\text{phen}^{\bullet-}$  modes. These occurred at  $1453$ ,  $1551$ , and  $1585 \text{ cm}^{-1}$ . The lowest energy band may be correlated to the band at  $1445 \text{ cm}^{-1}$  in the resonance Raman spectrum of  $[\text{Re}(\text{CO})_3(4\text{-Mepy})(\text{phen}^{\bullet-})]$

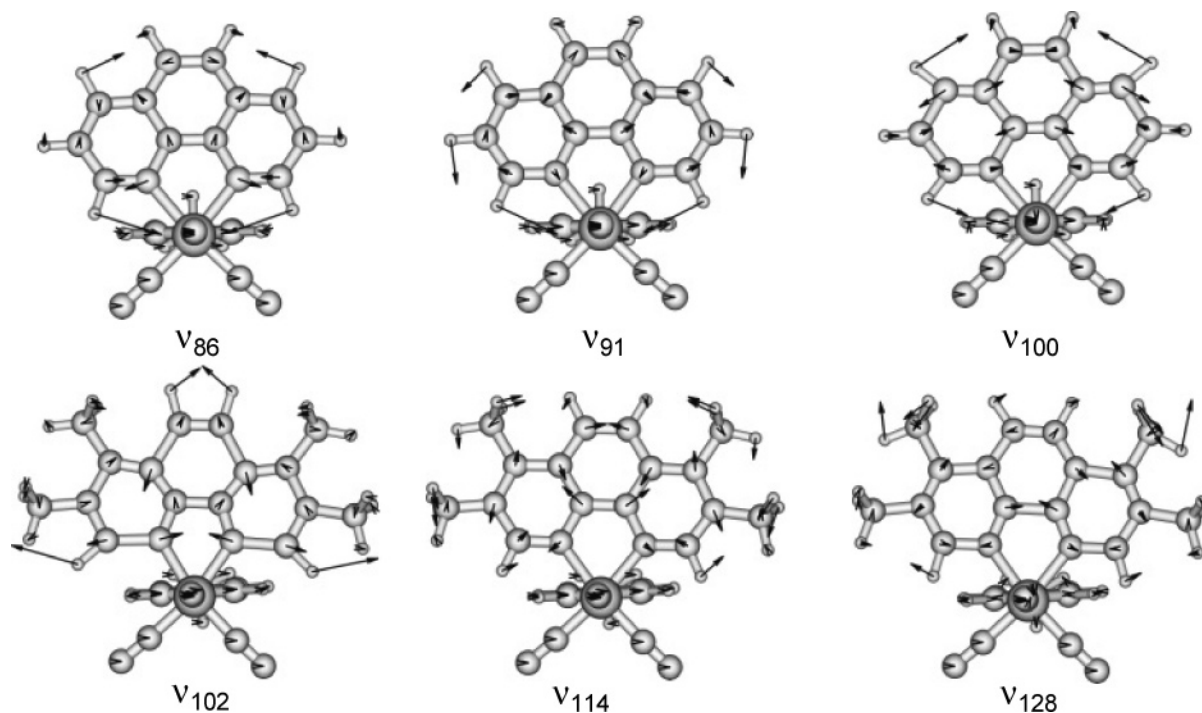


**Figure 5.** Eigenvectors for selected normal modes of  $[\text{Re}(\text{CO})_3(4\text{-Mepy})(\text{phen}^{\bullet-})]$  and  $[\text{Re}(\text{CO})_3(4\text{-Mepy})(\text{tem}^{\bullet-})]$ .

and the highest energy band correlated to one at  $1578\text{ cm}^{-1}$ . Although there is also a band at  $1511\text{ cm}^{-1}$  in the resonance Raman spectrum of  $[\text{Re}(\text{CO})_3(4\text{-Mepy})(\text{phen}^{\bullet-})]$ , this has been assigned as a 4-Mepy mode (vide supra).

The appropriateness of use of B3LYP/6-31G(d) (with LANL2DZ ECP for Re atoms) calculations for the polypyridyl ligand area of the vibrational spectra of Re(I) complexes was established by comparing the IR and Raman spectra of  $[\text{Re}(\text{CO})_3\text{Cl}(\text{phen})]$  and  $[\text{Re}(\text{CO})_3(4\text{-Mepy})(\text{phen})]^+$  to the frequencies calculated (see Supporting Information). For both complexes the mean absolute deviation between calculated and observed frequencies is  $5\text{ cm}^{-1}$ . Only small shifts in frequency ( $<7\text{ cm}^{-1}$ ) and relative intensities are observed for bands common to both complexes, suggesting that substitution of the  $\text{Cl}^-$  ligand for 4-Mepy causes little perturbation to the polypyridyl ligand.

DFT theory calculations have allowed the bands observed in the resonance Raman spectrum of  $[\text{Re}(\text{CO})_3(4\text{-Mepy})(\text{phen}^{\bullet-})]$  to be assigned. A number of bands are identified as 4-Mepy-localized modes. These appear at 1018, 1062, 1389, 1489, and  $1626\text{ cm}^{-1}$  in the resonance Raman spectrum and are calculated at  $1008\text{ }(\nu_{69})$ ,  $1064\text{ }(\nu_{72})$ ,  $1399\text{ }(\nu_{89})$ ,  $1471\text{ }(\nu_{97})$ ,  $1511\text{ }(\nu_{99})$ , and  $1626\text{ }(\nu_{105})\text{ cm}^{-1}$ , respectively. The remaining bands are assigned to  $\text{phen}^{\bullet-}$  localized modes. These occur at 1093, 1146, 1161, 1221, 1278, 1309, 1410, 1431, 1445, 1511, 1534, 1507, and  $1578\text{ cm}^{-1}$  (Table 2). Most of the bands observed are attributed to bands with  $a_1$  symmetry (assuming  $C_{2v}$  point group for phen). The exceptions are the bands at  $1278\text{ }(\nu_{85})$  and  $1410\text{ }(\nu_{90})\text{ cm}^{-1}$ , which have medium intensity at this excitation wavelength and are 4-Mepy- and phen-localized modes, respectively. The most intense band in the spectrum is observed at  $1534\text{ cm}^{-1}$ , predicted at  $1532\text{ cm}^{-1}\text{ }(\nu_{100})$ . This is a delocalized mode, involving atoms over the three rings in phen. Medium intensity bands observed at 1431 and  $1445\text{ cm}^{-1}$  are predicted at  $1421\text{ }(\nu_{91})$  and  $1460\text{ }(\nu_{95})\text{ cm}^{-1}$ , respectively.  $\nu_{91}$  can also be described as a delocalized phen mode, whereas  $\nu_{95}$  is based in the central ring of phen. The shifts observed on going from parent to reduced species are consistent with the population of a  $b_1$  SOMO.

The combination of IR and resonance Raman spectroscopy of the reduced complex, in concert with the DFT calculations support the assignment of the SOMO of  $[\text{Re}(\text{CO})_3(4\text{-Mepy})(\text{phen}^{\bullet-})]$  being  $b_1$  rather than  $a_2$  in nature.

Most of the bands in the resonance Raman spectrum of  $[\text{Re}(\text{CO})_3(4\text{-Mepy})(\text{tem}^{\bullet-})]$  have been assigned as  $\text{tem}^{\bullet-}$  based modes (Table 3). All have  $a_1$  symmetry, assuming  $C_{2v}$  symmetry of the phenanthroline moiety of the tem ligand. The mean absolute deviation, between calculated (B3LYP/6-31G(d)) and observed frequencies, is  $10\text{ cm}^{-1}$ . The bands at 1208 and  $1616\text{ cm}^{-1}$  have been assigned as 4-Mepy modes, predicted at  $1211\text{ }(\nu_{96})$  and  $1626\text{ }(\nu_{133})\text{ cm}^{-1}$ , respectively. The strongest bands in the region  $1000\text{--}1650\text{ cm}^{-1}$  are at 1307, 1427, and  $1444\text{ cm}^{-1}$ , predicted at  $1285\text{ }(\nu_{102})$ ,  $1435\text{ }(\nu_{114})$ , and  $1464\text{ }(\nu_{116})\text{ cm}^{-1}$ . The band at  $1444\text{ cm}^{-1}$ , which has been attributed to  $\nu_{116}$ , may actually be due to any or all of the four modes predicted between  $1464$  and  $1469\text{ cm}^{-1}$ .

As reduced  $[\text{Re}(\text{CO})_3(4\text{-Mepy})(\text{tem})]^+$  and  $[\text{Re}(\text{CO})_3(4\text{-Mepy})(\text{phen})]^+$  are both  ${}^2B_2$  species, it might be expected that they have bands in common due to the reduced phenanthroline moiety.

The bands at 1307, 1427, 1444, and  $1525\text{ }(\nu_{128})\text{ cm}^{-1}$  in the resonance Raman spectrum of  $[\text{Re}(\text{CO})_3(4\text{-Mepy})(\text{tem}^{\bullet-})]$  are also seen in the resonance Raman spectrum of  $[\text{Re}(\text{CO})_3(4\text{-Mepy})(\text{phen}^{\bullet-})]$  at 1309, 1431, 1445, and  $1534\text{ cm}^{-1}$ , respectively. The band at  $1534\text{ cm}^{-1}$  in the resonance Raman spectrum of  $[\text{Re}(\text{CO})_3(4\text{-Mepy})(\text{phen}^{\bullet-})]$  exhibits the largest shift from the phen to tem complex. This may be due to the change in character of the mode. In the phen complex, the mode is due to the phen moiety only, whereas in the tem complex there is some contribution to the mode from motion of atoms in the 4-Mepy ligand (Figure 5). Visualization of the modes reveals that  $\nu_{102}$  and  $\nu_{114}$ , of  $[\text{Re}(\text{CO})_3(4\text{-Mepy})(\text{tem}^{\bullet-})]$ , are delocalized over the three rings of the phenanthroline moiety of  $\text{tem}^{\bullet-}$  and involve some motion of the methyl groups in  $\text{tem}^{\bullet-}$ . The modes of  $[\text{Re}(\text{CO})_3(4\text{-Mepy})(\text{phen}^{\bullet-})]$  at 1309 and  $1431\text{ cm}^{-1}$  are delocalized over the three aromatic rings of phenanthroline.

## Conclusions

This study has shown that the nature of the acceptor molecular orbital of phenanthroline-based Re(I) complexes can be deduced from IR spectra by determining the  $\Delta k_{av}$  for the carbonyl bands upon reduction. These assignments have been supported by resonance Raman spectroelectrochemistry and DFT calculations, which have been used to investigate the polypyridyl ligand anion vibrational modes. DFT calculations predict the complexes considered as  ${}^2B_2$  species. The mean absolute deviation between calculated and observed vibrational frequencies in the 1000–1650  $\text{cm}^{-1}$  region was found to be 10  $\text{cm}^{-1}$ . The singly reduced  $[\text{Re}(\text{CO})_3\text{Cl}(\text{phen})]$ ,  $[\text{Re}(\text{CO})_3\text{Cl}(\text{dip})]$ ,  $[\text{Re}(\text{CO})_3\text{Cl}(\text{tem})]$ ,  $[\text{Re}(\text{CO})_3(4\text{-Mepy})(\text{phen})]^+$ , and  $[\text{Re}(\text{CO})_3(4\text{-Mepy})(\text{tem})]^+$  complexes were all found to be  ${}^2B_2$  species.

**Supporting Information Available:** Electronic absorption spectra of the reduction product of  $[\text{Re}(\text{CO})_3(4\text{-Mepy})(\text{phen})]^+$  and the reduction product of  $[\text{Re}(\text{CO})_3(4\text{-Mepy})(\text{tem})]^+$ . Table of calculated and observed vibrational frequencies of  $[\text{Re}(\text{CO})_3\text{Cl}(\text{phen})]$ . This material is available free of charge via the Internet at <http://pubs.acs.org>.

## References and Notes

- (1) Kalyanasundaram, K. *Photochemistry of Polypyridine and Porphyrin Complexes*; Academic Press: San Diego, 1992.
- (2) Endicott, J. F.; Uddin, M. J.; Schlegel, H. B. *Res. Chem. Intermed.* **2002**, *28*, 761.
- (3) Kaim, W. *J. Am. Chem. Soc.* **1982**, *104*, 3833.
- (4) Ernst, S.; Vogler, C.; Klein, A.; Kaim, W.; Zalis, S. *Inorg. Chem.* **1996**, *35*, 1295.
- (5) Farrell, I. R.; Hartl, F.; Zalis, S.; Mahabiersing, T.; Vlcek, A., Jr. *Dalton* **2000**, 4323.
- (6) Howell, S. L.; Gordon, K. C. *J. Phys. Chem. A* **2004**, *108*, 2536.
- (7) Farrell, I. R.; van Slageren, J.; Zalis, S.; Vlcek, A. *Inorg. Chim. Acta* **2001**, *315*, 44.
- (8) George, M. W.; Turner, J. J. *Coord. Chem. Rev.* **1998**, *177*, 201.
- (9) Matthewson, B. J.; Flood, A.; Polson, M. I. J.; Armstrong, C.; Phillips, D. L.; Gordon, K. C. *Bull. Chem. Soc. Jpn.* **2002**, *75*, 933.
- (10) Howell, S. L.; Matthewson, B. J.; Polson, M. I. J.; Burrell, A. K.; Gordon, K. C. *Inorg. Chem.* **2004**, *43*, 2876.
- (11) Lundin, N. J.; Walsh, P. J.; Howell, S. L.; McGarvey, J. J.; Blackman, A. G.; Gordon, K. C. *Inorg. Chem.* **2005**, *44*, 3551.
- (12) Walsh, P. J.; Gordon, K. C.; Lundin, N. J.; Blackman, A. G. *J. Phys. Chem. A* **2005**, *109*, 5933.
- (13) Moya, S. A.; Pastene, R.; Schmidt, R.; Guerrero, J.; Sartori, R. *Polyhedron* **1992**, *11*, 1665.
- (14) Oh, S. M.; Faulkner, L. R. *J. Am. Chem. Soc.* **1989**, *111*, 5613.
- (15) Fredericks, S. M.; Luong, J. C.; Wrighton, M. S. *J. Am. Chem. Soc.* **1979**, *101*, 7415.
- (16) Shriver, D. F.; Dunn, J. B. R. *Appl. Spectrosc.* **1974**, *28*, 319.
- (17) McCreery, R. L. *Raman Spectroscopy for Chemical Analysis*; John Wiley & Sons: New York, 2000.
- (18) The ASTM subcommittee on Raman spectroscopy has adopted eight materials as Raman shift standards (ASTM E 1840). The band wavenumbers for these standards are available at <http://chemistry.ohio-state.edu/~rmcreeer/shift.html>.
- (19) Babaei, A.; Connor, P. A.; McQuillan, A. J.; Umapathy, S. *J. Chem. Educ.* **1997**, *74*, 1200.
- (20) Waterland, M. R.; Gordon, K. C.; McGarvey, J. J.; Jayaweera, P. M. *J. Chem. Soc., Dalton Trans.* **1998**, 609.
- (21) Howell, S. L.; Scott, S. M.; Flood, A. H.; Gordon, K. C. *J. Phys. Chem. A* **2005**, *109*, 3745.
- (22) Frisch, M. J.; Trucks, G. W.; Schlegel, H. B.; Scuseria, G. E.; Robb, M. A.; Cheeseman, J. R.; Montgomery, J. A., Jr.; Vreven, T.; Kudin, K. N.; Burant, J. C.; Millam, J. M.; Iyengar, S. S.; Tomasi, J.; Barone, V.; Mennucci, B.; Cossi, M.; Scalmani, G.; Rega, N.; Petersson, G. A.; Nakatsuji, H.; Hada, M.; Ehara, M.; Toyota, K.; Fukuda, R.; Hasegawa, J.; Ishida, M.; Nakajima, T.; Honda, Y.; Kitao, O.; Nakai, H.; Klene, M.; Li, X.; Knox, J. E.; Hratchian, H. P.; Cross, J. B.; Bakken, V.; Adamo, C.; Jaramillo, J.; Gomperts, R.; Stratmann, R. E.; Yazyev, O.; Austin, A. J.; Cammi, R.; Pomelli, C.; Ochterski, J. W.; Ayala, P. Y.; Morokuma, K.; Voth, G. A.; Salvador, P.; Dannenberg, J. J.; Zakrzewski, V. G.; Dapprich, S.; Daniels, A. D.; Strain, M. C.; Farkas, O.; Malick, D. K.; Rabuck, A. D.; Raghavachari, K.; Foresman, J. B.; Ortiz, J. V.; Cui, Q.; Baboul, A. G.; Clifford, S.; Cioslowski, J.; Stefanov, B. B.; Liu, G.; Liashenko, A.; Piskorz, P.; Komaromi, I.; Martin, R. L.; Fox, D. J.; Keith, T.; Al-Laham, M. A.; Peng, C. Y.; Nanayakkara, A.; Challacombe, M.; Gill, P. M. W.; Johnson, B.; Chen, W.; Wong, M. W.; Gonzalez, C.; Pople, J. A. *Gaussian 03*, Gaussian, Inc.: Pittsburgh, PA, 2003.
- (23) Grills, D. C.; Turner, J. J.; George, M. W. Time-resolved infrared spectroscopy. *Comprehensive Coordination Chemistry II*; 2004; Vol. 2, p 91.
- (24) Schoonover, J. R.; Strouse, G. F.; Omberg, K. M.; Dyer, R. B. *Comments Inorg. Chem.* **1996**, *18*, 165.
- (25) Schoonover, J. R.; Bignozzi, C. A.; Meyer, T. J. *Coord. Chem. Rev.* **1997**, *165*, 239.
- (26) Braterman, P. S. *Metal carbonyl spectra*; Academic Press Inc. London Ltd, 1975.
- (27) Stor, G. J.; Hartl, F.; van Outersterp, J. W. M.; Stufkens, D. J. *Organometallics* **1995**, *14*, 1115.
- (28) Chen, P.; Palmer, R. A.; Meyer, T. J. *J. Phys. Chem. A* **1998**, *102*, 3042.
- (29) Baranovski, V. I.; Lubimova, O. O.; Makarov, A. A.; Sizova, O. V. *Chem. Phys. Lett.* **2002**, *361*, 196.
- (30) The  $b_1$  LUMO of phen has no electron density on at the C5 and C6 positions. This molecular orbital only has density on the bpy moiety of phen.
- (31) George, M. W.; Johnson, F. P. A.; Westwell, J. R.; Hodges, P. M.; Turner, J. J. *J. Chem. Soc., Dalton Trans.* **1993**, 2977.
- (32) Klein, A.; Kaim, W.; Waldhoer, E.; Hausen, H.-D. *J. Chem. Perkin Trans.* **1995**, 2121.
- (33) Klein, A.; McInnes, E. J. L.; Kaim, W. *J. Chem. Soc., Dalton Trans.* **2002**, 2371.
- (34) Scott, A. P.; Radom, L. *J. Phys. Chem.* **1996**, *100*, 16502.
- (35) Kalyanasundaram, K. *J. Chem. Soc., Faraday Trans. 2* **1986**, *82*, 2401.
- (36) Turro, C.; Chung, Y. C.; Leventis, N.; Kuchenmeister, M. E.; Wagner, P. J.; Leroi, G. E. *Inorg. Chem.* **1996**, *35*, 5104.
- (37) Schoonover, J. R.; Omberg, K. M.; Moss, J. A.; Bernhard, S.; Malueg, V. J.; Woodruff, W. H.; Meyer, T. J. *Inorg. Chem.* **1998**, *37*, 2585.
- (38) The electronic absorption spectrum of phen $^{\cdot-}$  has been previously reported and there are a number of bands.<sup>39,40</sup> As a lithium salt in THF, these lie at 394, 582 and 631 nm with a shoulder at 538 nm as reported by Schoonover et al.<sup>37</sup> Our electronic absorption spectrum of  $[\text{Re}(\text{CO})_3(4\text{-Mepy})(\text{phen}^{\cdot-})]$  has a broad absorption in the visible with a shoulder at ~540 nm and extensive absorption out to 650 nm. The resonance Raman data we report are in resonance with the low energy shoulder rather than the stronger 390 nm band. In our case measurements within the higher energy chromophore would be complicated by the fact that the parent species also absorbs and thus gives resonance Raman scattering at those shorter wavelengths.
- (39) Kato, T.; Shida, T. *J. Am. Chem. Soc.* **1979**, *101*, 6869.
- (40) Malueg, V. J. M.A. Thesis, University of Texas at Austin, 1981.